HAL
open science

Photoinduced Persistent Electron Accumulation and Depletion in LaAlO 3 / SrTiO 3 Quantum Wells

Yu Chen, Yoann Lechaux, Blai C Casals, Bruno Guillet, Albert Minj, Jaume Gazquez, Laurence Méchin, Gervasi C Herranz

To cite this version:

Yu Chen, Yoann Lechaux, Blai C Casals, Bruno Guillet, Albert Minj, et al.. Photoinduced Persistent Electron Accumulation and Depletion in LaAlO 3 / SrTiO 3 Quantum Wells. Physical Review Letters, 2020, 124 (24), 10.1103/physrevlett.124.246804 . hal-02906097

HAL Id: hal-02906097

https://hal.science/hal-02906097v1

Submitted on 4 Jan 2021

HAL is a multi-disciplinary open access archive for the deposit and dissemination of scientific research documents, whether they are published or not. The documents may come from teaching and research institutions in France or abroad, or from public or private research centers.

L'archive ouverte pluridisciplinaire **HAL**, est destinée au dépôt et à la diffusion de documents scientifiques de niveau recherche, publiés ou non, émanant des établissements d'enseignement et de recherche français ou étrangers, des laboratoires publics ou privés.

Photoinduced Persistent Electron Accumulation and Depletion in $LaAlO_3/SrTiO_3$ Quantum Wells

Yu Chen,[1] Yoann Lechaux,[2] Blai Casals,[1,†] Bruno Guillet,[2] Albert Minj,[2,3] Jaume Gázquez,[1] Laurence Méchin,[2] and Gervasi Herranz[1,*]

[1]*Institut de Ciència de Materials de Barcelona (ICMAB-CSIC), Campus UAB, 08193 Bellaterra, Catalonia, Spain*
[2]*Normandie Univ, UNICAEN, ENSICAEN, CNRS, GREYC, 14000 Caen, France*
[3]*IMEC, Kapeldreef 75, Leuven 3000, Belgium*

(Received 27 January 2020; accepted 14 May 2020; published 19 June 2020)

Persistent photoconductance is a phenomenon found in many semiconductors, by which light induces long-lived excitations in electronic states. Commonly, persistent photoexcitation leads to an increase of carriers (accumulation), though occasionally it can be negative (depletion). Here, we present the quantum well at the $LaAlO_3/SrTiO_3$ interface, where in addition to photoinduced accumulation, a secondary photoexcitation enables carrier depletion. The balance between both processes is wavelength dependent, and allows tunable accumulation or depletion in an asymmetric manner, depending on the relative arrival time of photons of different frequencies. We use Green's function formalism to describe this unconventional photoexcitation, which paves the way to an optical implementation of neurobiologically inspired spike-timing-dependent plasticity.

DOI: 10.1103/PhysRevLett.124.246804

In many semiconductors, photoexcitation of DX centers leads to long-term changes of conductance, caused by the long decay of excited carriers to the ground state [1–7]. In most cases, photoexcitation drives carrier accumulation, while in other few cases, as reported for graphene [8], persistent photoconductance can be negative. Yet, a simultaneous control of persistent accumulation and depletion in a quantum well (QW) by optical means has remained elusive.

Here, we present a quantum well, where in addition to carrier accumulation, a secondary photoexcitation couples to QW states via quantum tunneling, enabling carrier depletion. The system under study is the interface between two wide-band-gap insulators, $SrTiO_3$ and $LaAlO_3$, where an electronic reconstruction, driven by electrostatic boundary conditions, leads to the formation of the QW [9,10] [Figs. 1(a) and 1(b)]. The possibility of tunable carrier accumulation and depletion opens up interesting perspectives, including the use of these QWs for the implementation of artificial optical synapses or spin-charge conversion modulated by light.

To explain the unconventional phototransport of the $LaAlO_3/SrTiO_3$ interface, we propose two processes leading, respectively, to the increase or decrease of the QW occupancy. First, we argue that carrier accumulation is caused by photoexcitation of DX-center states, conventionally regarded as responsible for persistent photoconductance in many semiconductors [1,5,26,27]. DX centers are point defects—either interstitials or vacancy complexes—that couple strongly to the lattice via electron-phonon interaction [1,5]. Consequently, their energetics requires the configurational coordinate space, with lattice deformations described by Q. Depending on their charge state, DX centers form either a shallow level with equilibrium point $Q_0 = 0$ or a deeper level that deforms the lattice locally ($Q_0 \neq 0$) and traps electrons. Figure 1(c) plots the dependence on Q of the conduction band $E_{CB}(Q)$ and DX-center states $E_c(Q)$ [described by Eqs. (2) and (3) below]. The presence of an energy barrier E_b precludes carriers excited to $E_{CB}(Q)$ to return to the DX-center state, causing long-term accumulation in the QW.

Alternatively, a second photoexcitation path leads to carrier depletion. Briefly, $LaAlO_3$ is a polar material with a built-in electric field that needs compensation to reach stability [28,29]. Below a critical thickness ($t_c \approx 1.5$ nm), the interface is insulating and counteracting dipoles created by charged surface and interface states balance the internal electric field [30] [Fig. 1(a)], while at thickness t_c, the field compensation is achieved by the transfer of carriers from surface states to the $LaAlO_3/SrTiO_3$ interface forming the QW [31] [Fig. 1(b)]. Therefore, a perturbation of this electrostatic balance generates an uncompensated internal electric field ΔE inside $LaAlO_3$ that drives changes in the QW population. This explains the observed conductance modulation caused by changes in the surface chemistry using scanning probe methods [32] or by solvent immersion [33,34]. Our work reveals that photoexcitation at resonant wavelengths also modifies the charge of surface states, leading to carrier depletion.

An intuitive way to understand carrier depletion is as follows. A DX center distorts the lattice and phonons vibrate around a shifted equilibrium point [35]:

 © 2020 American Physical Society

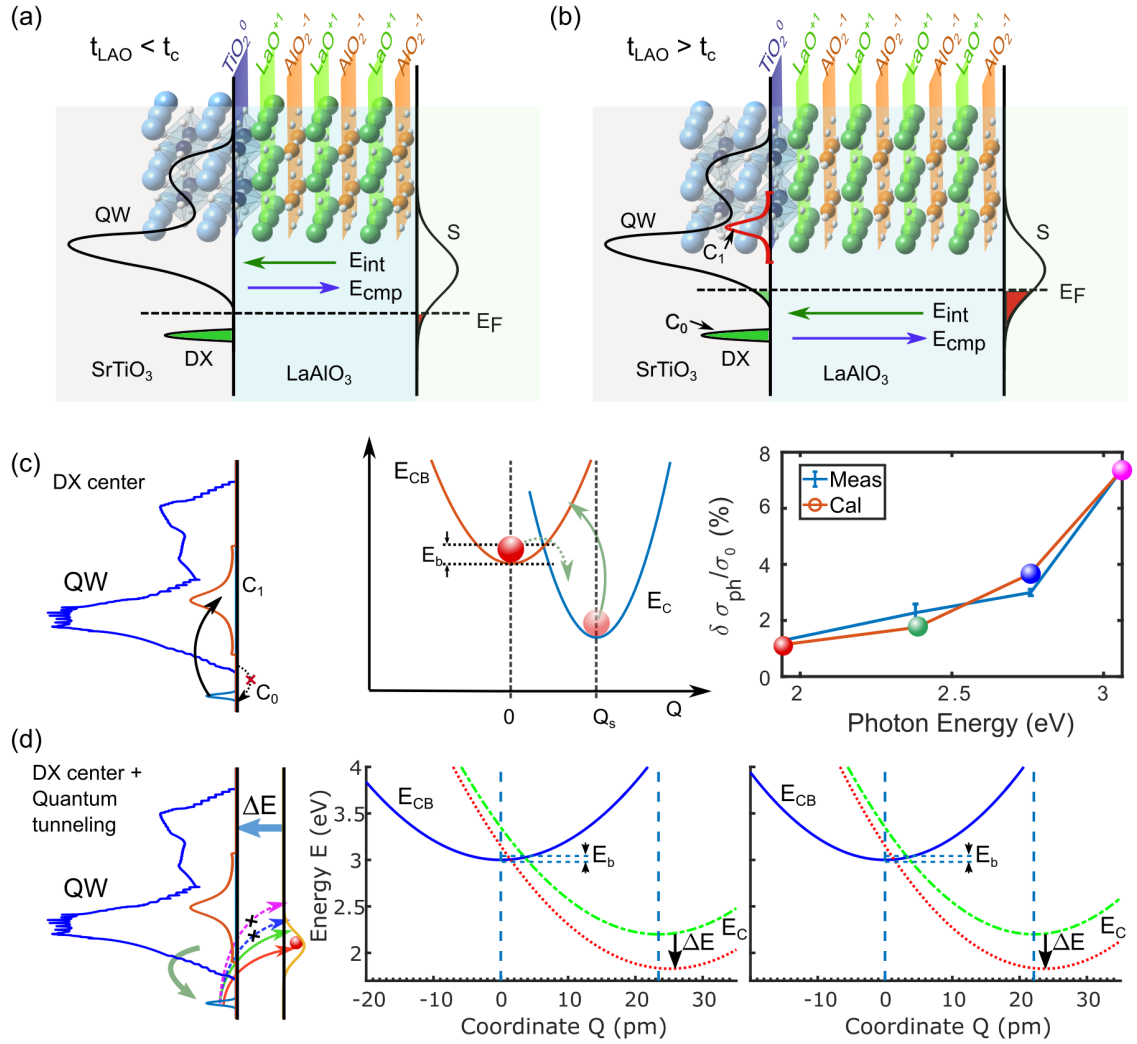

FIG. 1. Photoexcitation of carriers into or out of the quantum well (QW). (a) Charged atomic planes in $LaAlO_3$ $[(LaO)^+/(AlO_2)^-]$ drive an internal electric field E_{int} compensated by the field E_{cmp} created by interface DX centers and surface states (S). (b) Above t_c, electrons transfer from the surface to the QW. (c) Carrier accumulation into the QW proceeds via photoexcitation of DX centers, see left panel. Initially, a DX center (c_0) traps carriers, which are promoted to the QW through the excitation of the DX-center (c_1). As shown in the middle panel, they are not allowed to jump back to c_0 because of the energy barrier (E_b) caused by differences in the configurational coordinate (Q). Right panel shows that DX-center photoexcitation based on the model described by Eq. (4) predicts correctly the spectral dependence of the photoconductance $\delta\sigma_{ph}/\sigma_0$ (see also Note S5 in the Supplemental Material [11]). (d) As sketched in the left panel, resonant photoexcitation to surface states triggers carrier depletion. This causes an unbalanced internal field that shifts the $E_c(Q)$ band. We calculate this shift using Eqs. (2) and (3), assuming longitudinal optical (LO) modes $\hbar\omega_q \approx 58.5$ meV (middle panel) and $\hbar\omega_q \approx 62$ meV (right), corresponding, respectively, to $SrTiO_3$ [24] and $LaAlO_3$ [25], (see Note S6 in Supplemental Material [11] for more details).

$$Q_0 \approx M_q \left(\frac{\hbar}{2M\omega_q}\right)^{1/2}, \tag{1}$$

$$E_{CB}(Q) = E_{CB,0} + \frac{1}{2}M\omega_q^2 Q^2, \tag{2}$$

$$E_c(Q) = E_{c_0} + \frac{1}{2}M\omega_q^2 Q^2 + B[V_{DX} + E_{ext}]Q + [V_{DX} + E_{ext}], \tag{3}$$

where M is the ionic mass density, M_q is the electron-phonon coupling constant, $\hbar$ the Planck's constant, and ω_q is the frequency of a normal lattice mode. The shifted equilibrium position generates a polarized distortion that can couple to an unbalanced internal electric field ΔE created by photoexcitation across the $LaAlO_3$ barrier. We describe this coupling by the following equations [36]:

where $E_{CB,0}$, E_{c_0} are reference energy levels, $\frac{1}{2}M\omega_q^2 Q^2$ is the kinetic energy of vibrating ions of reduced mass M, V_{DX} is the DX-center trapping potential, B couples

electrostatic terms to lattice deformations, and $E_{\mathrm{ext}} = e\Delta E t_{\mathrm{LAO}}$, is the energy linked to the unbalanced electric field ΔE created by resonant photoexcitation to surface states (t_{LAO} is the thickness of $LaAlO_3$). Figure 1(d) plots $E_{\mathrm{CB}}(Q)$ and $E_c(Q)$ for compensated ($\Delta E = 0$) and uncompensated ($\Delta E \neq 0$) fields. We observe that $\Delta E \neq 0$ pushes $E_c(Q)$ to lower energies, decreasing the energy barrier E_b. This enables the return of excited carriers to the DX center, causing photoinduced carrier depletion. Multiphonon emission or absorption allows energy changes associated with the photoexcitation and deexcitation of carriers [36].

We have therefore two mechanisms that predict opposite effects on the conductance, as long as there is a resonant photoexcitation to surface states that enables carrier depletion. We have checked this hypothesis in $LaAlO_3/SrTiO_3$ by measuring the photoresponse at different wavelengths. In particular, Fig. 2(a) shows that the conductance measured after a first pulse of red light ($\lambda_1 = 638$ nm) followed by a second pulse of blue light ($\lambda_2 = 450$ nm), increases the conductance. However, when we invert the pulse timing, we observe that the conductance resets to the initial value [Fig. 2(a)], indicating that photoexcitation with red light promotes carrier depletion. Figure 2(b) displays phototransport measurements measured at different wavelengths, showing that photoexcitation to surface states is resonant around $\lambda = 638$ nm. Interestingly, sequences of multiple short- or long-frequency pulses enable dynamic carrier accumulation and depletion, as shown in Fig. 2(c).

Two further experiments confirm the relevance of electrostatic boundary conditions. First, uncompensated internal fields cannot happen in amorphous $LaAlO_3$ layers, because of the lack of well-defined atomic planes. In this case, oxygen vacancies, rather than electronic reconstruction, drive metallicity in amorphous $LaAlO_3/SrTiO_3$ interfaces [37]. Therefore, in this case, resonant surface photoexcitation cannot cause carrier depletion. We checked this prediction by measuring the photoconductance of devices defined on interfaces between amorphous $LaAlO_3$ films ($t \approx 3$ nm) and $SrTiO_3$ [see Figs. 3(a), 3(b)]. The experiment, shown in the right panel of Fig. 3(c), confirms that carrier depletion is absent in this case.

A second proof relies on the fact that quantum tunneling decays exponentially with barrier thickness, so that depletion caused by resonant excitation to surface states should drop as the thickness of epitaxial $LaAlO_3$ increases. To verify it, we measured the conductance change after photoexcitation with red light in devices defined with variable $LaAlO_3$ thickness. Left and middle panels of Fig. 3(c) display the results for $t \approx 5$ uc ≈ 1.9 nm and $t \approx 14$ uc ≈ 5.3 nm. We observe that, while the conductance decreases noticeably at $t \approx 5$ uc, it does not appreciably change for $t \approx 14$ uc. This observation confirms that the increase of $LaAlO_3$ thickness reduces drastically quantum tunneling to surface states, disabling the mechanism for carrier depletion.

We describe quantitatively the two photoexcitation processes by defining in-scattering $\Sigma_{\mathrm{in}}(\vec{x}, t)$ and out-scattering $\Sigma_{\mathrm{out}}(\vec{x}, t)$ functions that give account of the inward and outward flux of particles in the QW. Using Green's function formalism, we derive the following expressions (see Supplemental Material [11] for details on this derivation):

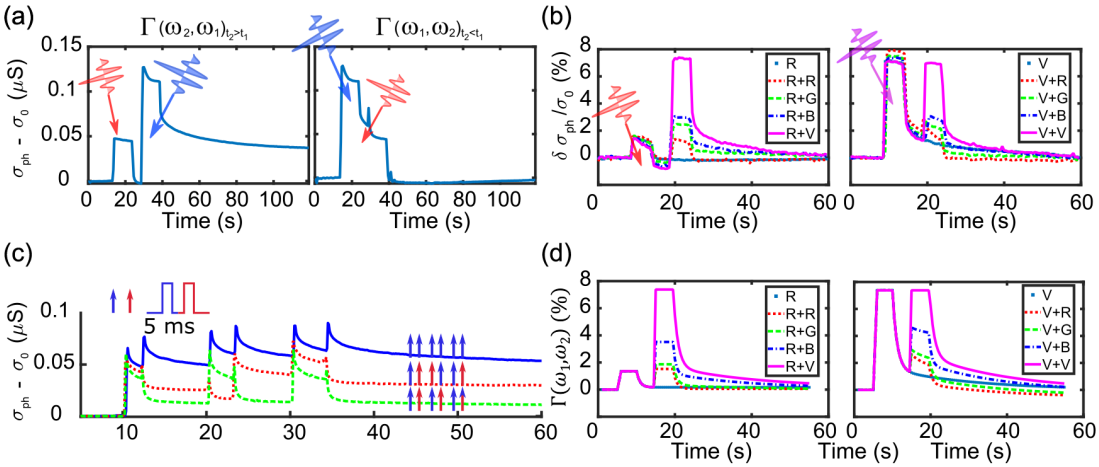

FIG. 2. (a) Photoexcitation combining blue and red pulses with opposite time sequences. When the second pulse is red, the conductance *decreases* to the initial value prior to excitation, displaying photoinduced carrier depletion. (b) Left: photoconductance measured after a red pulse followed by green, blue, and violet pulses. In all cases, there is an increase of conductance after the second pulse. Right: after a first violet pulse, the depletion after the second pulse is strongest with red, and negligible for blue. (c) Relative changes of conductance after different multiple-pulse sequences. The blue curve corresponds to changes induced by an all-blue-pulse sequence, while red and green curves correspond to multiple blue or red-pulse sequence. The whole sequence shows that the plastic increase or decrease of conductance depends on the time order of arrival of pulses of different frequencies. (d) Numerical calculations of the photoconductance based on the function $\Gamma(\omega_1, \omega_2) = [\Sigma_{\mathrm{in}}(\omega_1, \omega_2) + \Sigma_{\mathrm{out}}(\omega_1, \omega_2)]$ described in the main text (see Supplemental Material [11] for details).

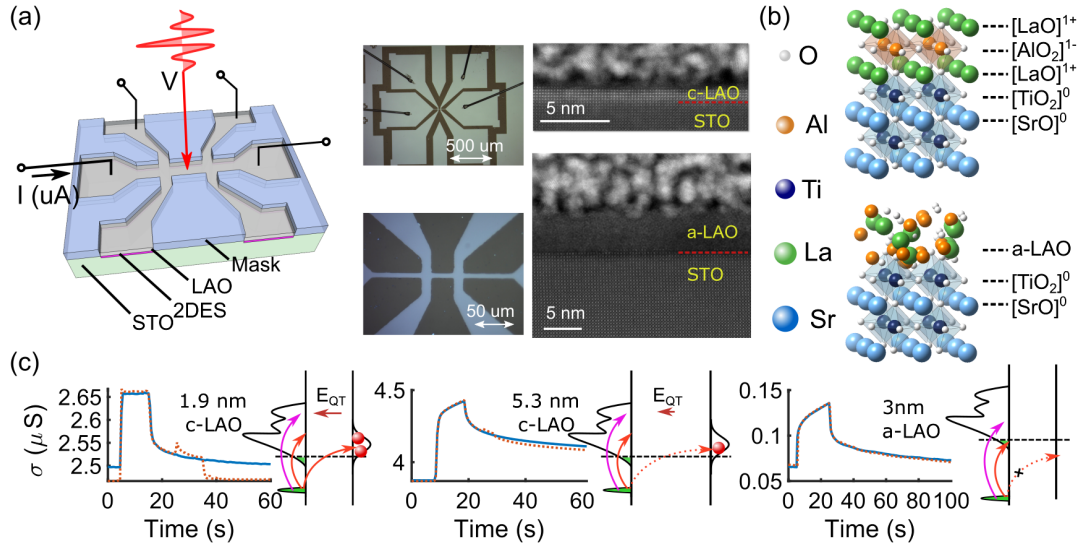

FIG. 3. Electrostatic boundary conditions and carrier depletion. (a) We designed Hall devices, pictured here, to measure the photoconductance. We fabricated devices with epitaxial (c-LAO) and amorphous (a-LAO) $LaAlO_3$ layers (the right panels display cross-sectional scanning transmission electron microscopy (STEM) images taken across the channel of measured Hall devices). We show that carrier depletion via quantum tunneling photoexcitation only occurs in epitaxial $LaAlO_3$ barriers while it is absent in amorphous layers due to the lack of an internal electric field in the latter. In (b) we show a schematic depiction of atomic arrangements of epitaxial (top) and amorphous (bottom) layers. (c) Illumination with blue plus red pulses induces carrier depletion in the sample with thin epitaxial $LaAlO_3$ ($t = 5$ uc ≈ 1.9 nm). However, the depletion is much smaller when the thickness increases to $t = 14$ uc ≈ 5.3 nm, due to the fast decrease of quantum tunneling of photoexcited carriers. Likewise, carrier depletion is absent in the sample with amorphous $LaAlO_3$ layer. Therefore, carrier depletion via quantum tunneling photoexcitation requires thin epitaxial layers of $LaAlO_3$.

$$\Sigma_{\rm in}(\omega) \propto P\frac{\pi}{\omega}\left[\int\int \delta\{\hbar\omega - (\varepsilon^*_{DX} - \varepsilon_{DX})\}(1 - n^*_{DX}(\varepsilon^*_{DX}))n_{DX}(\varepsilon_{DX})d\varepsilon_{DX}d\varepsilon^*_{DX}\right]e^{-g(2N_q+1)} \times \sum_m \delta\{\hbar(\omega - \omega_m)I_m(\gamma)\}e^{m\hbar\omega_q/2k_BT}, \tag{4}$$

$$\Sigma_{\rm out}(\omega) \propto I_{I-S} = 4\pi e T_0 \int d\varepsilon n_i(\varepsilon)n_s(\varepsilon + \hbar\omega). \tag{5}$$

Equation (4) describes carrier accumulation, where ω is the frequency of light, P is the transition matrix element, assumed to be energy independent, k_B the Boltzmann's constant, $n^*_{\rm DX}(\varepsilon^*_{\rm DX})$ and $n_{\rm DX}(\varepsilon_{\rm DX})$ are, respectively, the density of states of ground and excited DX-center states, g is the electron-phonon coupling, and $N_q = [e^{\hbar\omega_q/k_BT} - 1]^{-1}$ is phonon occupation assuming an Einstein model with ω_q. From Eq. (4) we see that photoexcitation of DX centers involves around m phonons, so that $\hbar\omega_m = \varepsilon^*_{\rm DX} - \varepsilon_{\rm DX} - (g - m)\hbar\omega_q$. Consequently, the amplitude of this transition is modulated by m, described by the Bessel function $I_m(\gamma)$, where $\gamma = 2g\sqrt{N_0(N_0 + 1)}$. On the other hand, Eq. (5) describes depletion by resonant photoexcitation, where I_{I-S} is the net current from interface to surface states, e is the electron charge, ε is the energy, n_s is the density of surface states, T_0 is the tunneling parameter, assumed to be independent of ε, and ω is the frequency of light.

Figure 2(d) displays the values of the function $\Gamma(\omega_1,\omega_2) = [\Sigma_{\rm in}(\omega_1,\omega_2) + \Sigma_{\rm out}(\omega_1,\omega_2)]$, which describes the net change of QW occupancy by adding up the in-scattering and out-scattering contributions after two-pulse photoexcitation with frequencies ω_1, ω_2. We observe that the calculated $\Gamma(\omega_1,\omega_2)$ curves reproduce accurately the photoresponse measured under different pulse combinations and, in particular, describe carrier depletion induced by the resonant photoexcitation.

We stress that alternative models that do not rely on DX centers fail to reproduce the observed spectral photoresponse [see note S5 in Ref. [11] and Fig. 1(c)]. This observation begs the question about the origin of DX centers in this system. In this regard, several works have studied the energetics of defects in $LaAlO_3/SrTiO_3$. For instance, $[{\rm Al_{Ti}}(I)/{\rm Ti_{Al}}(S)]$ pairs, where (I) stands for the interface and (S) the surface, are deep levels that trap

electrons [30]. Alternatively, Al-rich $LaAlO_3$ layers are necessary to generate the QW [38,39], where the excess aluminum substitutes for lanthanum [39], which could also form midgap states. In this regard, our DLTS (deep-level transient spectroscopy) study reveals electron trapping centers around 0.8 eV below the conduction band [11], which could be related to the aforementioned defects. On the other hand, oxygen vacancies at the $LaAlO_3$ surface [30] could be at the origin of resonant photoexcitation, while other studies indicate that surface protonation induced by light contribute also to photoconductance [40]. In view of all these considerations, the full identification of DX centers and resonant surface states remains open and requires further work.

Before concluding, we note that while persistent photoconductance has general interest for optoelectronic applications [8], the asymmetric photoexcitation observed here is reminiscent of STDP (for spike-timing dependent plasticity) observed in neurobiological systems [41,42], so far physically implemented in memristor devices [43,44]. The sensitivity to time correlations in optical inputs [see Fig. 2(c)] is a basic feature of STDP and opens an interesting perspective on the use of optical synapses based on photoconductive QWs [45], as discussed by us recently [46]. Alternatively, in the light of our observations, we envisage using optical pulses to modulate other $LaAlO_3/SrTiO_3$ QW properties, e.g., the amplitude and sign of the recently observed spin-charge conversion [47].

This work was supported by the Spanish Ministerio de Ciencia, Innovación y Universidades through Grants No. MAT2017-85232-R (AEI/FEDER,EU) and Severo Ochoa SEV-2015-0496 and the Generalitat de Catalunya through Grant No. 2017 301 SGR1377. Y. L., B. G., and L. M. acknowledge the Normandy region and European Regional Development Fund through the projects RIN RECHERCHE PLACENANO Contract No. 18E01664/18P02478 and RIN RECHERCHE EVOL_PELIICAEN Contract No. 17P04260/17P04263. Y. C. acknowledges the China Scholarship Council Grant No. 201506890029. J. G. acknowledges Ramón y Cajal (RyC) contract (2012-11709). The STEM microscopy work was conducted in the ICTS-CNME. STEM-specimen preparation was conducted in "Laboratorio de Microscopias Avanzadas" at the Instituto de Nanociencia de Aragon-Universidad de Zaragoza. The authors acknowledge both the ICTS-CNME and the LMA-INA for offering access to their instruments and expertise. We acknowledge collaboration and discussions with Dr. Florencio Sánchez regarding thin film growth.

*Corresponding author.
gherranz@icmab.cat
†Present address: Department of Earth Sciences, University of Cambridge, Downing Street, Cambridge CB2 3EQ, United Kingdom.

[1] D. V. Lang and R. A. Logan, Phys. Rev. Lett. **39**, 635 (1977).
[2] J. C. Bourgoin and A. Mauger, Appl. Phys. Lett. **53**, 749 (1988).
[3] T. N. Morgan, Semicond. Sci. Technol. **6**, B23 (1991).
[4] T. Ihn, *Semiconductor Nanostructures: Quantum States and Electronic Transport* (Oxford University Press, Oxford, 2010).
[5] S. Lany and A. Zunger, Phys. Rev. Lett. **100**, 016401 (2008).
[6] M. C. Tarun, F. A. Selim, and M. D. McCluskey, Phys. Rev. Lett. **111**, 187403 (2013).
[7] D. Eom, C.-Y. Moon, and J.-Y. Koo, Nano Lett. **15**, 398 (2015).
[8] C. Biswas, F. Güneş, D. D. Loc, S. C. Lim, M. S. Jeong, D. Pribat, and Y. H. Lee Nano Lett. **11**, 4682 (2011).
[9] A. Ohtomo and H. Y. Hwang, Nature (London) **427**, 423 (2004).
[10] N. Reyren *et al.* Science **317**, 1196 (2007).
[11] See Supplemental Material at http://link.aps.org/supplemental/10.1103/PhysRevLett.124.246804 for a detailed description of the Hamiltonians, simulations, and experimental methods, which includes Refs. [12–23].
[12] E. Simoen, J. Lauwaert, and H. Vrielinck, Semicond. Semimet. **91**, 205 (2015).
[13] J. V. Li and G. Ferrari. *Capacitance Spectroscopy of Semiconductors* (Pan Stanford, Singapore, 2018).
[14] P. Coleman, *Introduction to Many-Body Physics*, 1st ed. (Cambridge University Press, Cambridge, England, 2016).
[15] T. Wolfram and S. Ellialtıoğlu, *Electronic and Optical Properties of d-Band Perovskites* (Cambridge University Press, Cambridge, England, 2006).
[16] T. Wolfram, Phys. Rev. Lett. **29**, 1383 (1972).
[17] M. Breitschaft, V. Tinkl, N. Pavlenko, S. Paetel, C. Richter, J. R. Kirtley, Y. C. Liao, G. Hammerl, V. Eyert, T. Kopp, and J. Mannhart, Phys. Rev. B **81**, 153414 (2010).
[18] K. Yang, S. Nazir, M. Behtash, and J. Cheng, Sci. Rep. **6**, 34667 (2016).
[19] A. F. Santander-Syro *et al.* Nature (London) **469**, 189 (2011).
[20] Z. S. Popović, S. Satpathy, and R. M. Martin, Phys. Rev. Lett. **101**, 256801 (2008).
[21] W. J. Son, E. Cho, B. Lee, J. Lee, and S. Han, Phys. Rev. B **79**, 245411 (2009).
[22] S. T. Hartman, B. Mundet, J. C. Idrobo, X. Obradors, T. Puig, J. Gazquez, and R. Mishra, Phys. Rev. Mater. **3**, 114806 (2019).
[23] T. L. Meyer, H. Jeen, X. Gao, J. R. Petrie, M. F. Chisholm, and H. N. Lee, Adv. Electron. Mater. **2**, 1500201 (2016).
[24] J. Petzelt, T. Ostapchuk, I. Gregora, I. Rychetsky, S. Hoffmann-Eifert *et al.* Phys. Rev. B **64**, 184111 (2001).
[25] M. V. Abrashev, A. P. Litvinchuk, M. N. Iliev, R. L. Meng, V. N. Popov,V. G. Ivanov, R. A. Chakalov, and C. Thomsen, Phys. Rev. B **59**, 4146 (1999).
[26] C. Wetzel, T. Suski, J. W. Ager, E. R. Weber, E. E. Haller, S. Fischer, B. K. Meyer, R. J. Molnar, and P. Perlin, Phys. Rev. Lett. **78**, 3923 (1997).
[27] T. Thio, J. W. Bennett, D. J. Chadi, R. A. Linke, and M. C. Tamargo, J. Electron. Mater. **25**, 229 (1996).
[28] N. Nakagawa, H. Y. Hwang, and D. A. Muller, Nat. Mater. **5**, 204 (2006).

[29] J. Gazquez, M. Stengel, R. Mishra, M. Scigaj, M. Varela, M. A. Roldan, J. Fontcuberta, F. Sanchez, and G. Herranz, Phys. Rev. Lett. **119**, 106102 (2017).
[30] L. Yu and A. Zunger, Nat. Commun. **5**, 5118 (2014).
[31] S. Thiel, G. Hammerl, A. Schmehl, C. W. Schneider, and J. Mannhart. Science **313**, 1942 (2006).
[32] C. Cen, S. Thiel, G. Hammerl, C. W. Schneider, K. E. Andersen, C. S. Hellberg, J. Mannhart, and J. Levy Nat. Mater. **7**, 298 (2008).
[33] Y. Xie, Y. Hikita, C. Bell, and H. Y. Hwang, Nat. Commun. **2**, 494 (2011).
[34] A. Keith *et al.* Nat. Commun. **7**, 10681 (2016).
[35] G. D. Mahan, *Many-Particle Physics* (Springer-Verlag New York Inc., United States, 2007).
[36] C. H. Henry and D. V. Lang, Phys. Rev. B **15**, 989 (1977).
[37] Y. Chen, N. Pryds, J. E. Kleibeuker, G. Koster, J. Sun, E. Stamate, B. Shen, G. Rijnders, and S. Linderoth, Nano Lett. **11**, 3774 (2011).
[38] E. Breckenfeld, N. Bronn, J. Karthik, A. R. Damodaran, S. Lee, N. Mason, and L. W. Martin, Phys. Rev. Lett. **110**, 196804 (2013).
[39] M. P. Warusawithana *et al.* Nat. Commun. **4**, 2351 (2013).
[40] K. A. Brown *et al.*, Nat. Commun. **7**, 10681 (2016).
[41] C. Zamarreño-Ramos, L. A. Camuñas-Mesa, J. A. Pérez-Carrasco, T. Masquelier, T. Serrano-Gotarredona, and B. Linares-Barranco Front. Neurosci. **5**, 26 (2011).
[42] S. Saïghi *et al.* Front. Neurosci. **9**, 51 (2015).
[43] S. Boyn *et al.* Nat. Commun. **8**, 14736 (2017).
[44] Z. Wang *et al.* Nat. Mater. **16**, 101 (2017).
[45] O. Bichler, D. Querlioz, S. J. Thorpe, J.-P. Bourgoin, and C. Gamrat. Neural Netw. **32**, 339 (2012).
[46] Y. Chen, B. Casals, F. Sánchez, and G. Herranz. ACS Appl. Electron. Mater. **1**, 1189 (2019).
[47] D. C. Vaz *et al.*, Nat. Mater. **18**, 1187 (2019).